ELSEVIER

Polymer 43 (2002) 4315–4323

polymer

www.elsevier.com/locate/polymer

Poly(styrene-*b*-isobutylene-*b*-styrene) block copolymer ionomers (BCPI), and BCPI/silicate nanocomposites. 1. Organic counterion: BCPI sol–gel reaction template

Kenneth A. Mauritz[a,*], Robson F. Storey[a], David A. Mountz[a], David A. Reuschle[b]

[a]*Department of Polymer Science, The University of Southern Mississippi, Southern Station Box 10076, Hattiesburg, MS 39406-0076, USA*
[b]*The Dow Chemical Company, 2301 Brazosport Boulevard, B-1470, Freeport, TX 77541, USA*

Received 15 October 2001; received in revised form 5 April 2002; accepted 8 April 2002

Abstract

Silicate structures were inserted along the cylindrical polystyrene (PS) domains in an ionomer form of elastomeric poly(styrene-*b*-isobutylene-*b*-styrene) tri-block copolymers, via in situ sol–gel reactions. Environmental scanning electron microscopy/energy dispersive X-ray spectroscopy studies indicated that silicate structures do in fact grow within the interior of ca. 0.8 mm thick films rather than forming undesirable silica precipitates on the surface. The combination of a domain-selective swelling solvent (DMAc) and the attachment of large organic counterions (benzyltrimethylammonium) along the styrene blocks facilitated the preferential migration of hydrolyzed $Si(OEt)_4$ monomers to these ionic domains where the sol–gel reactions are apparently seeded. Differential scanning calorimetry and dynamic mechanical studies indicated that T_g for the polyisobutylene (PIB) phase is essentially unaffected, but the PS phase T_g shifts to higher values with ionomer formation, and to even higher values with subsequent silicate phase insertion. These two methods provide indirect evidence that the silicate component is mainly incorporated in the PS rather than PIB domains. Combined with the results of earlier atomic force microscopy studies that demonstrated that the basic morphology of the unmodified block copolymer is unchanged despite the insertion of a silicate phase, the data presented here reinforce the concept of a robust sol–gel reaction template. Also, the rubbery plateau storage modulus was elevated as a result of ionomer formation and more so after the ionomer was imparted with a silicate phase, which illustrates mechanical reinforcement. © 2002 Elsevier Science Ltd. All rights reserved.

Keywords: Block copolymer ionomer template; Sol–gel reactions; Ionomer/silicate nanocomposite

1. Introduction

Mauritz et al. created a variety of [organic polymer]/[inorganic oxide] nanocomposites via polymer-in situ sol–gel polymerizations of metal alkoxide and organo-alkoxysilane monomers [1–7]. In one of these cases, it was demonstrated that the quasi-ordered phase-separated morphology of Nafion® perfluorosulfonate ionomers can act as a 3D template for these sol–gel polymerizations [1]. 'Template', in this particular context, refers to the targeted growth of inorganic oxide or organically modified silicate structures within a specific nanostructured polymer phase based on the miscibility of the alkoxide monomer, or its hydrolyzed versions, within this phase. In the case of Nafion®, it appears that sol–gel reactions of sorbed, hydrolyzed alkoxides are confined to the regions consisting of aggregates of the long sulfonate-terminated sidechains [8].

In the work reported here, we expand this theme and provide evidence that the distinct phase-separated morphology of poly(styrene-*b*-isobutylene-*b*-styrene) (PS–PIB–PS) block copolymer ionomers (BCPI) can also be used as a morphological template for sol–gel reactions involving tetraethylorthosilicate (TEOS) monomers, thereby creating novel organic–inorganic hybrid materials. BCPI swelling agents that facilitate the selective migration of hydrolyzed TEOS monomers to the ionic styrene domains, where the sol–gel reactions are seeded, are critical. The compatibility of the hydrolyzed TEOS monomers with the PS domains is also controlled by the nature of the cation. This process is depicted in simple fashion in Fig. 1. The specific goal of this work was to selectively insert polar, hydrophilic silicate structures along the hard cylindrical PS domains in ionomer forms of this block copolymer (BCP).

It should be mentioned that other investigators have used phase-separated block copolymers as templates in the sense of in situ, domain-targeted growth of organic and inorganic nanoscopic structures. de Jesus and Weiss polymerized

---

* Corresponding author. Tel.: +1-601-266-5595; fax: +1-601-266-5635.
E-mail address: kenneth.mauritz@usm.edu (K.A. Mauritz).

0032-3861/02/$ - see front matter
PII: S0032-3861(02)00261-6

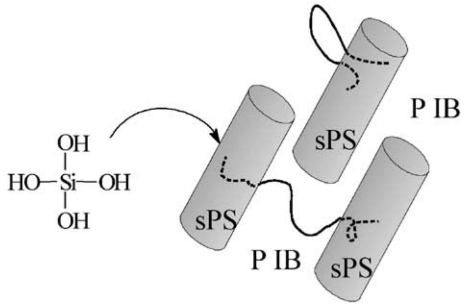

Fig. 1. Depiction of PS domain—targeted silicate formation via BCPI—in situ sol–gel reactions for hydrolyzed TEOS. The PS domains are sulfonated and neutralized with cations.

pyrrole within the lamellar microdomains of sulfonated poly(styrene-*b*-(ethylene-*alt*-propylene)) diblock copolymers [9]. Ishizu et al. inserted colloidal silver by the reduction of sorbed silver ions into the lamellae of quarternized poly(styrene-*b*-2 vinylpyridine) diblock copolymers [10]. Chen et al. constructed [*four-arm star* styrene–butadiene block copolymer *elastomer*]/silicate hybrid materials via an in situ sol–gel process for TEOS in the pre-formed polymer, and it was concluded that bonded silicate structures resided in the polystyrene (PS) domains [11]. Huang et al. grew TiO_2–SiO_2 structures in elastomeric styrene-*b*-[ethylene-*ran*-butylene]-*b*-styrene block copolymers via in situ sol–gel reactions between TEOS and tetrabutyltitanate [12]. In this latter study, the hard blocks were amino-functionalized and subsequent reactions between these groups and glycidyloxypropyl trimethoxysilane provided chemical coupling between the polymer and TiO_2–SiO_2 phases, although there appeared to be no template effect with regard to a targeted dispersion of the sol–gel-derived phase. Ikeda et al. performed sol–gel reactions for TEOS in cross-linked styrene–butadiene rubbery block copolymers, but templating did not occur and the size of the silicate particles was simply governed by cross-link density [13]. Templin et al. grew organically modified aluminosilicate mesostructures in poly(isoprene-*b*-ethylene oxide) block copolymers [14]. Here, the polymer-in situ sol–gel polymerizations appeared to templated as the polyethylene oxide blocks served as anchors for the metal alkoxide condensation products.

The equilibrium morphologies of linear (PS block)-(soft block) copolymers are usually such that PS cylinders occur in the approximate PS composition range corresponding to ca. 20–40% volume fraction. Elastomeric PS–PIB–PS block copolymers having comonomer compositions that yield cylindrical morphologies were synthesized in this work using controlled living carbocationic polymerization. The PS blocks in these BCPs were sulfonated; then the sulfonic acid groups were converted to the benzyltrimethylammonium ($BTMA^+$)-sulfonate form. The use of this large organic cation, in conjunction with the BCPI swelling agent DMAc, generated a templated nanocomposite morphology when the ionomer films were subjected to in situ sol–gel reactions for TEOS. DMAc was chosen to selectively swell the ionic PS domains in the BCPI based on the fact that this solvent will dissolve pure PS, but not a PIB homopolymer. DMAc-swollen films were immersed in sol–gel reactive TEOS solutions, while $(EtO)_{4-x}Si(OH)_x$ monomers diffused into the ionic PS regions where the condensation reactions in the following scheme are assumed to take place:

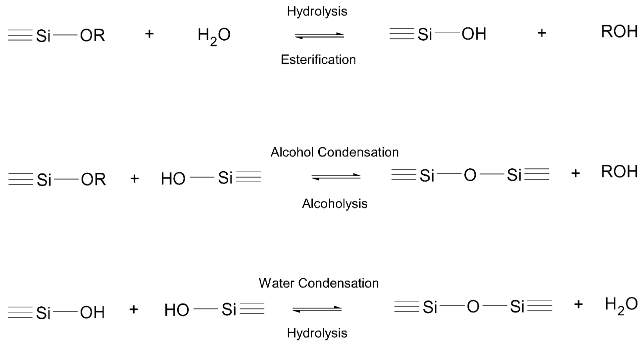

Beyond the initial reactions between monomer units, reactions of monomers with larger silicic acid oligomers as well as between silicic acid monomers take place so that, ultimately, extended gel-like structures form and these solvent-imbibed structures solidify upon sample drying. The simple sol–gel process that occurs in *bulk* reaction vessels usually involves a solution of water, an acid or base catalyst, an alkoxysilane monomer, and a solvent in which the alkoxysilane monomer and water are mutually miscible [15]. The main factors affecting sol–gel reactions and the resultant amorphous structures are the mole ratio H_2O/SiOR, solution pH, reaction time, temperature, and drying conditions after the onset of gelation [16]. However, when sol–gel reactions take place within polymers, the influence of these variables can be altered or complicated by the interactions and constraints posed by the polymer matrix, especially within phase-separated polymers. Moreover, the thickness of BCPI films will affect the ultimate distribution of silicate structures owing to diffusion limitations on hydrolyzed TEOS molecules.

Earlier atomic force microscopy (AFM) [17] and small angle X-ray scattering (SAXS) [18] studies involving the PS–PIB–PS-based hybrids revealed a composite morphology consisting of rods that are structured in essentially parallel hexagonal arrays. Fig. 2 is a tapping mode-phase image of a $BTMA^+$ BCPI (BCP $M_w = 76\,900\ g\ mol^{-1}$, 18 mol% PS of which 16 mol% is sulfonated) that contains 6.5 wt% silicate as the result of in situ sol–gel reactions for TEOS. The center–center inter-rod distances in this image are in the order of tens-of-nanometers. The SAXS studies of the PS–PIB–PS-based materials reinforced the conclusions derived from the AFM experiments and showed that the inter-rod spacing increased with the insertion of the silicate phase.

The important conclusion of these past structural studies is that the phase-separated morphology of the unfilled

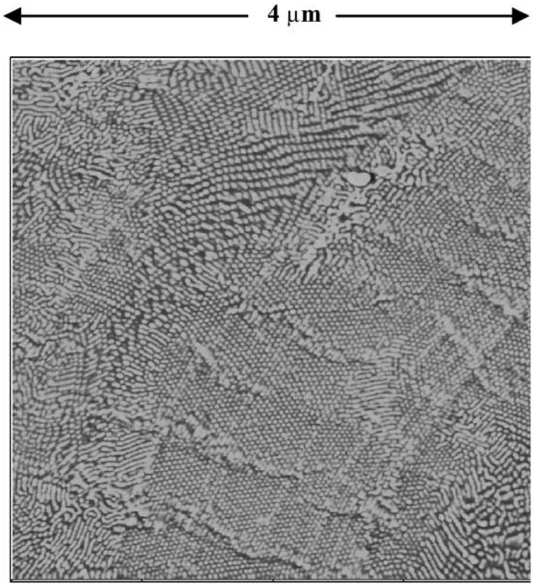

Fig. 2. Tapping mode-phase image of a BCPI incorporating 6.5% silicate. $M_w = 76\ 900$ g mol^{-1} and there is 18 mol% PS of which 16 mol% is sulfonated and then ion exchanged with BTMA cations. The image is 4 μm × 4 μm full scale. Figure taken from Ref. [9].

ionomer is preserved despite its invasion by the in situ-grown, sol–gel-derived silicate phase. Furthermore, sulfonation and ion exchange of the parent BCP does not change the inter-rod spacing. This result is in contrast with the work of Weiss et al. who studied sulfonated commercial SEBS (Kraton®) materials that are similar to our experimental PS–PIB–PS materials [19]. These investigators found that the extent of microphase separation was in fact influenced by ionic aggregation in the PS domains. Weiss et al. also reported that the sulfonation and neutralization of di- and tri-block copolymers of PS and poly(ethylene-*alt*-propylene) hindered the development of a well-ordered morphological texture relative to the parent block copolymers [20]. It might be envisioned that sulfonation might increase the volume fraction of the PS phase or/and strong electrostatic interactions might affect a morphological shift, although this is not the case for the materials discussed here.

Here, the details of the stepwise preparation of these nanocomposites are reported. Also discussed are the results of the characterization of these materials using the techniques of environmental scanning electron microscopy/energy dispersive X-ray spectroscopy (ESEM/EDS), differential scanning calorimetry (DSC), and dynamic mechanical analysis (DMA). DMA and DSC can provide evidence of whether the silicate in-growths intrude within the PIB phase to a significant degree, or are mainly confined to the sulfonated styrenic regions by observing the regions of the glass transition of the PIB and PS domains. The rationale behind this view is that silicate structures that significantly penetrate a given phase would alter long range chain segmental mobility therein.

2. Experimental

2.1. Block copolymer synthesis and characterization

A 20 g batch of PS–PIB–PS was synthesized by a sequential living cationic polymerization. A combination of 1,3-di(2-chloro-2-propyl)-5-*tert*-butylbenzene and $TiCl_4$ was used as the initiating system. The polymerization was done using pyridine as an electron donor and di-*tert*-butyl pyridine as a proton trap in 60/40 (v/v) hexane/methyl chloride cosolvents at −80 °C. Further details of the synthesis are reported elsewhere [21–23].

The molecular weight and molecular weight distribution of the PIB middle block as well as the entire block copolymer was determined by the use of gel permeation chromatography (GPC). The GPC system that was employed consisted of an Alcott model 728 autosampler, a Waters model 510 solvent delivery system, a Waters model 410 differential refractometer, a Waters model 484 tunable ultraviolet detector that was operating at 256 nm, a Wyatt Technology miniDAWN® on-line multi-angle laser light scattering detector and two Polymer Laboratories 5μ mixed-D columns that were thermostated to 30 °C. Tetrahydrofuran (THF), freshly distilled from CaH_2, was employed as the mobile phase and was delivered at a flow rate of 1.0 ml/min. Sample concentrations were approximately 4 mg/ml with an injection loop volume of 110 μl.

^{1}H NMR spectroscopy was used to measure the PS weight fraction by comparing the integrated areas under the aliphatic and aromatic regions of the spectra as described previously [22]. The PS volume fraction was calculated for the BCP using the densities 1.06 and 0.92 g/cm^3 for PS and PIB, respectively. Spectra were obtained using a 200 MHz Bruker NMR spectrometer. Samples were analyzed as 10% (w/v) solutions in $CDCl_3$, using tetramethylsilane as an internal reference.

2.2. Reagents

All reagents that were involved beyond the stage of block copolymer synthesis were used without further purification. TEOS (98%), *n*-hexanol (98%), tetrachloroethylene (99%), *p*-toluenesulfonic acid monohydrate (98.5 + %), BTMA hydroxide (40 wt% in methanol), and dichloroethane (99%) were obtained from Aldrich Chemical Co. 1,4-Dioxane (ACS grade), 1-propanol (certified), THF (99.9%), methanol (99.9%), acetic anhydride (ACS grade), *N*,*N*-dimethylacetamide (DMAc, 99%) and sulfuric acid (ACS grade) were from Fisher Co.

2.3. Block copolymer sulfonation

Sulfonation of the BCP was performed using a procedure described by Weiss et al. [24]. The BCP was dissolved in dichloroethane and then acetyl sulfate (1.0 M) was added to the solution. The reaction was terminated after 2 h by stream stripping the sulfonated block copolymer (sBCP). The precipitate was washed with acetone and dried at 50 °C under vacuum until the mass of the precipitate remained constant.

Mole percent sulfonation was determined by dissolving approximately 0.5 g of sBCP in 100 ml toluene and 1 ml *n*-hexanol. The solution was heated to 80 °C (±2 °C) and titrated to a phenolthalein endpoint using 0.0211N BTMA hydroxide in methanol. The BTMA solution was standardized against solutions of *p*-toluenesulfonic acid. The mole percent sulfonate content of the block copolymer was found to be 16%. The accuracy of the titration procedure was verified by elemental analysis done by Atlantic Microlabs (Norcross, GA) and the average difference between the sulfonation values measured by these two techniques was seen to be less than 2%.

2.4. Ionomer formation

Neutralization of the sulfonated BCP to form an ionomer was carried out by titration of a 85:15 v/v solution of tetrachloroethylene (TCE)/hexanol and the sulfonic acid functionalized BCP with BTMA hydroxide base to create the $BTMA^+$ form [25]. A methanolic solution of BTMA hydroxide was added to a solution of the sBCP at 80 °C to affect an ion exchange reaction. Films were cast from these solutions onto the surfaces of Teflon® pans. The pans were put in a drying oven at 60 °C under an atmosphere of nitrogen for 13 days. The films were then annealed for 1 day at 60 °C, 1 day at 130 °C, and 9 h at 150 °C. All annealing steps were done under vacuum. The films had an average thickness of 0.8 mm, were free of surface texture and voids, were transparent and had a light yellow-brown color.

2.5. BCPI in situ sol–gel reactions and BCPI/silicate hybrid material formation

The dried $BTMA^+$ BCPI films were swollen in DMAc so as to have a weight gain of around 100% and these swollen films were introduced to flasks in which there were sol–gel reaction conditions for TEOS. Typical reaction conditions were as follows. A solution of 80 ml DMAc, 64 ml TEOS and 20 ml acidified water (pH ~ 1.2) was prepared in a separate flask and swirled until it appeared homogeneous, i.e. miscible. These concentrations are such that the H_2O/TEOS mole ratio is 4:1. The solvent-swollen BCPI film was then placed in the sol–gel reaction flask for prescribed times on the order of minutes. According to the sol–gel polymerization template hypothesis, the hydrolyzed TEOS monomers will selectively migrate to the ionic PS block domains. TEOS uptake increases with time in the reactor and the sol–gel reaction continues after the film is removed. Silicate uptake increases with the degree of BCPI pre-swelling in DMAc. The films were gently swirled in the sol–gel reactor to keep fresh solution in contact with its surface. Afterward, the films were removed and rinsed with absolute ethanol to remove possible surface precipitates, blotted with a tissue and then placed on a non-stick surface. Then, the sample was transferred to a vacuum oven at 100 °C to remove solvent and further drive condensation reactions of residual SiOH groups and this temperature was maintained for 1 day. After this, the temperature was raised to, and held at 120 °C for 1 day. Finally, the temperature was raised to 160 °C for ~6 h to remove residual solvent. The sample weight does not decrease beyond this time. The vacuum oven was then allowed to cool to room temperature, after which the films were removed for analysis. The mass of the BCPI film was determined by gravimetric means before and after the in situ sol–gel reaction followed by film drying. The weight percent uptake was calculated as [(composite mass − unfilled BCPI mass)/unfilled BCPI mass] × 100%.

It was discovered using ESEM/EDAX that most if not all of the silicate component exists in the form of surface-attached layers on the acid form BCP films when they are immersed in TEOS sol–gel reaction baths. Owing to the fact that these samples are not true composites, only the ionomer forms were used as sol–gel polymerization templates to form (PS–PIB–PS)/silicate nanocomposites.

Temperature changes under sol–gel reaction conditions. A little-discussed consideration with regard to polymer-in situ sol–gel reactions involves the change in temperature as the reaction proceeds. Even the sol–gel process for the less-reactive TEOS monomers can generate heat, which can raise the solution temperature to a considerable degree. While it would be difficult to track the instantaneous temperature within a polymer in which sol–gel reactions are evolving, it is instructive to note the magnitude of this phenomenon within a simple bulk solution using the same solvent, H_2O/TEOS ratio, and catalyst. While the interactions and constraints within a polymer matrix are more complex, a rough estimate of the temperature changes can be made. This information is relevant with regard to whether or not the temperature excursion overlaps a transition temperature of the polymer, such as T_g of the PS domains.

Eighty milliliter of DMAc was combined with 64 ml of TEOS and 20 ml of acidified water (pH 1.2). This solution swirled vigorously in a 250 ml Erlenmeyer flask until it appeared clear. The temperature of the DMAc and TEOS liquids prior to mixing was 22 °C. A simple thermometer was placed in this solution and temperature recorded vs. time.

2.6. Environmental scanning electron microscopy/energy dispersive X-ray spectroscopy

An ElectroScan E20 ESEM instrument with a Tracor-Noran Series II EDS system was used to inspect the surfaces and cross-sections of BCPI/silicate films to obtain a view of the spatial dispersion of the silicate phase. Owing to the magnitude of typical hemispherical sample-beam interaction volumes for back-scattered electrons and X-rays (several microns), the spots analyzed were separated by tens-of-microns. Other factors, such as pressure in the specimen chamber, sample working distance, and filament type will also affect the spatial resolution of spots analyzed using an EDS detector and it is possible that some of the X-rays analyzed from one spot may overlap to a neighboring spot. The spots analyzed were in the order of tens-of-microns apart.

Of primary concern in these experiments was the question of whether the sol–gel reactions for TEOS did in fact occur within the bulk of the film as opposed to causing an undesirable precipitation of a pure silica layer on the film surface. To answer this question, EDS elemental analyses were conducted at several points in cross-sections along a line perpendicular to the film surface to determine the ratio of silicon-to-sulfur X-ray counts, Si/S. This ratio normalizes the quantity of Si to the number of $-SO_3^-$ groups at a given point. Si/S plotted with respect to depth into the film is referred to as a silicon compositional profile. Although the results should not be viewed as being more than semi-quantitative, it is stressed that the main goal was to ascertain whether silicate structures have primarily formed within the bulk of the film.

2.7. Differential scanning calorimetry

DSC experiments were conducted using a Mettler thermal analysis work station. Data were collected with a DSC 30 and TC 15 controller. First and second heating scans were run from −150 to 200 °C at 10 °C/min although the thermograms are displayed over a smaller range to focus on the transitions of interest. T_g is taken here as the minimum on the first derivative DSC curve, which corresponds to the inflection point on the second heating trace. The inflection points of the PIB phase transition are listed in Table 2.

2.8. Dynamic mechanical analysis

DMA experiments were conducted on a selected BCP, a $BTMA^+$ BCPI derived from this parent BCP, and a BCPI/silicate nanocomposite using a TA Instruments DMA system, Model 2980. Test specimens consisted of films having a thickness of ~0.8 mm and the gauge length was 10 mm. The temperature was increased, starting from −120 to above 100 °C, at a rate of 3 °C/min while cyclic tensile data was collected at a fixed frequency of 1 Hz.

3. Results and discussion

3.1. PS–PIB–PS parent block copolymer molecular weight

The number and weight average molecular weights, polydispersity indices, and styrene compositions of the block copolymers used in these experiments are listed in Table 1.

Table 1
Block copolymer number and weight average molecular weight (M_n and M_w, respectively), mole and wt% PS, and polydispersity index (PDI = M_w/M_n) of PS–PIB–PS samples listed in the order of increasing percent PS

Sample	M_n/M_w	PDI	Mole/wt% PS
A	47 200/55 400	1.17	3.0/5.7
B	47 000/57 500	1.22	9.5/16.2
C	66 300/72 300	1.09	11.0/18.4
E	56 200/59 900	1.07	13.0/21.5
F	65 300/75 100	1.15	13.0/21.9
H	62 200/76 900	1.24	17.3/27.9
I	62 800/78 400	1.25	17.7/28.5

3.2. Temperature changes under sol–gel reaction conditions

A significant increase in the temperature of the bulk sol–gel reaction medium upon combination of the reactants is seen in Fig. 3. The initially cloudy solution became clear after about 3 min of mixing when the solution temperature was 36 °C. The solution temperature reached a maximum of 47 °C and then slowly decreased as heat was lost to the surroundings owing to the fact that this experiment was not performed under adiabatic conditions. The temperature levels off after about seven and one-half minutes. This simple experiment shows that a significant temperature change, up to +25 °C, can occur while comiscibility occurs between TEOS, water and DMAc and the hydrolysis and condensation reactions proceed in acid catalyzed fashion. The maximum temperature of 47 °C is significantly lower than T_g for the PS block domains so that heat transfer from the reactants to the polymer template will not cause major structural re-ordering.

3.3. ESEM/EDS studies of Si/S compositional profiles

Fig. 4 shows an ESEM micrograph of a BCPI/silicate composite of indicated composition as well as the associated Si/S compositional profile. The film is mounted on edge. This sample was freeze-fractured by its immersion into liquid nitrogen and then it was cracked. The rough appearance of the fracture surface might be reflective of

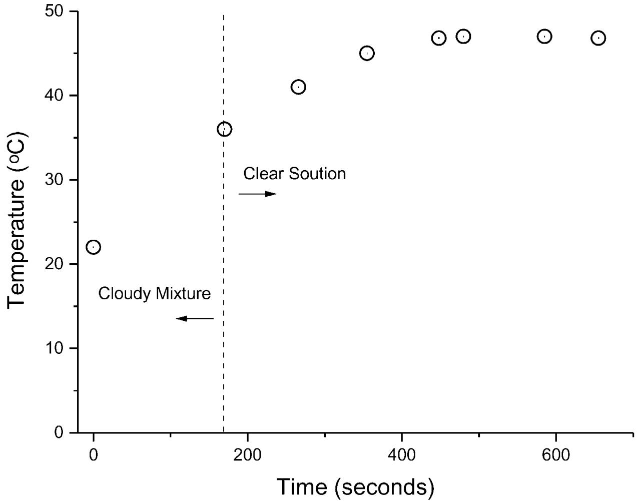

Fig. 3. Temperature vs. sol–gel reaction time for a bulk mixture of TEOS, acidified water, and DMAc.

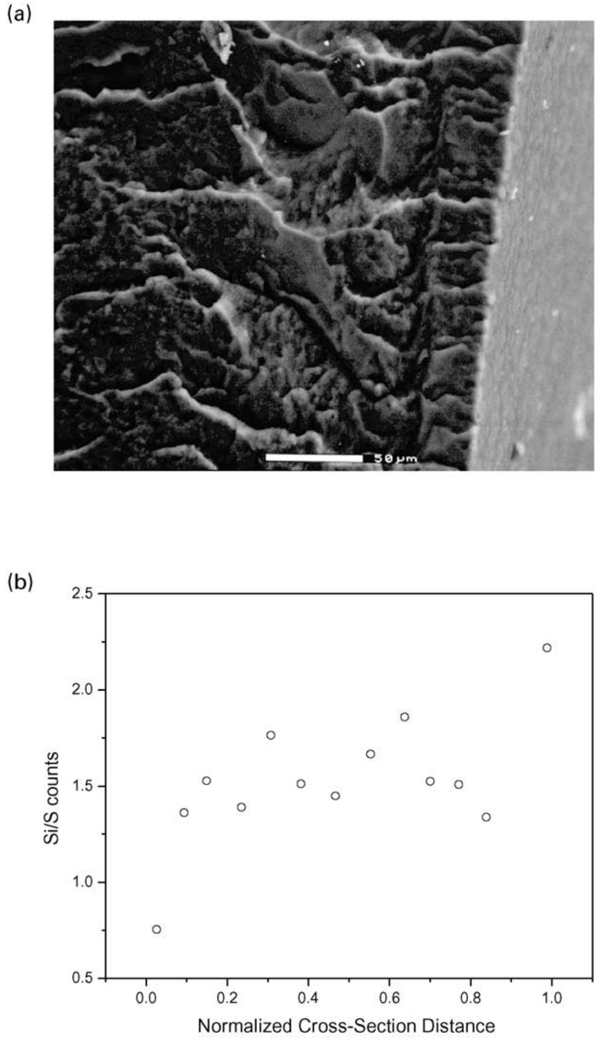

Fig. 4. (a) ESEM micrograph, showing a region of a freeze fracture—produced cross-section near an edge of a $BTMA^+$ BCPI/(6.5% silicate) film. The composition of the parent BCP is: $M_w = 76\ 900\ \mathrm{g\ mol^{-1}}$ and 27.9 wt% PS, of which 16 mol% is sulfonated. (b) EDS Si/S profile across the thickness direction of the same film. The horizontal axis is labeled in terms of relative film depth, and the extreme positions 0.0 and 1.0 correspond to the two film surfaces.

mechanical toughness as imparted by a reinforcing silicate phase. The external film surface is to the right of the edge seen in the right half of the micrograph. An important conclusion is that no precipitation of silica appears on the smooth external film surface. However, this is not the case for the sulfonic acid form. The EDS Si/S profile suggests that a silicate phase is distributed somewhat uniformly across the thickness direction. Importantly, a silicate component was able to penetrate and deposit entirely across the interior of this film, which is nominally 0.5 mm thick, during the time of the experiment, which was 1 h.

3.4. DSC studies of unmodified block copolymers

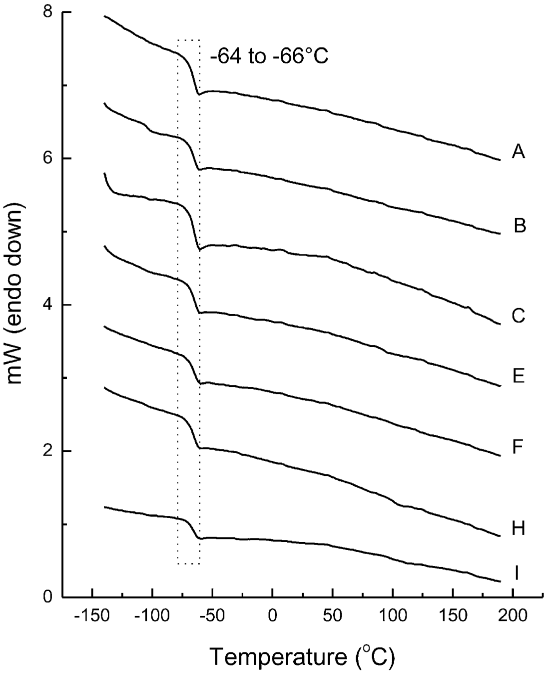

Fig. 5. Second scan DSC thermograms for the parent BCPs where the PIB phase glass transition breadth, of around 13 °C, is bracketed. The PS phase glass transition, at around 100 °C, is too weak to be clearly visible.

The DSC curves for the unsulfonated BCP samples listed in Table 1 are shown in Fig. 5. It is seen in Table 2 that the PIB phase T_g occurs at around −65 °C for all of the BCPs, regardless of molecular weight or PS block size. T_g is taken to be the temperature corresponding to the well-defined minimum in the first derivative curves. This value is in the vicinity of T_g for a pure PIB homopolymer [26]. While the molecular weights for these samples do not lie over a particularly broad range, percent styrene does vary over a significant range. A glass transition in the region for pure PS (~100 °C) is not apparent, although glass transitions that are weak or invisible on DSC traces are often seen using DMA, which, will be seen later in this report.

3.5. DSC studies of sBCPs, $BTMA^+$ form BCPIs and $BTMA^+$ BCPI/silicate composites

T_g for the acid form is essentially the same as that for the

Table 2
PIB phase T_g (defined as the inflection point) for the unmodified block copolymers as determined from second scan DSC thermograms. Two replicate samples are listed to demonstrate data reproducibility

Sample	Run 1 T_g	Run 2 T_g	Styrene (wt%)	M_w ($\mathrm{g\ mol^{-1}}$)
A	− 65.2	− 65.3	5.7	55 400
B	− 65.5	− 65.5	16.2	57 500
C	− 65.3	− 65.3	18.4	72 300
E	− 64.8	− 65.0	21.5	59 900
F	− 65.2	− 64.0	21.9	75 100
H	− 65.8	− 65.0	27.9	76 900
I	− 65.0	− 64.8	28.5	78 400

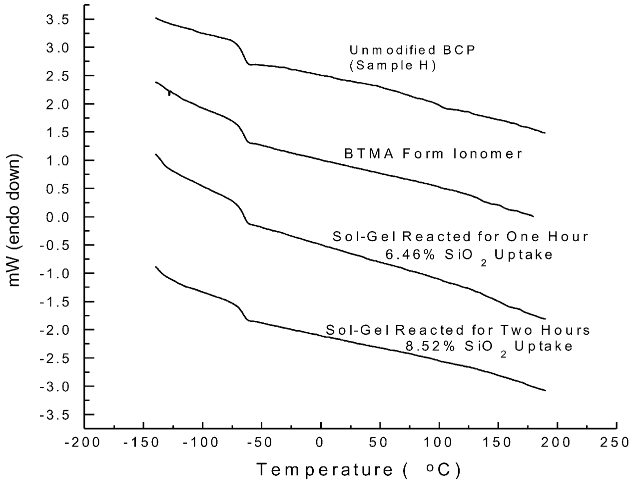

Fig. 6. Second scan DSC thermograms of a parent BCP, a BTMA$^+$ ionomer form of the same BCP, and two TEOS-reacted samples of the same BTMA$^+$ BCPI that had undergone in situ sol–gel reactions for the different indicated times.

corresponding unsulfonated sample in both cases, which suggests that styrene block sulfonation does not affect PIB block segmental mobility for these compositions. As mentioned earlier, true composites based on the acid form were not achieved because the silicate component exists in the form of silica deposits on the membrane surfaces rather than being dispersed throughout the inside of the membranes.

The DSC thermograms of an unmodified BCP, a BTMA$^+$ BCPI form of the same BCP, and two BTMA$^+$ BCPI/silicate composites that were formed from this ionomer that had silicate uptakes of 6.5 and 8.5 wt%, are shown in Fig. 6. There is a faint vestige of the glass transition for the unmodified BCP at around 100 °C but this feature is not seen on the thermograms for the modified forms. In Table 3, it is seen that there is little change in the PIB block T_g with respect to either BTMA$^+$ ionomer formation or subsequent silicate incorporation in this ionomer to the extent of having 6.5 and 8.5% uptake.

These facts are in harmony with the concept that chain segmental mobility in the rubbery PIB phase is largely unperturbed by the incorporation of a silicate component with the strong suggestion that the silicate structures would prefer to organize in or around the PS domains.

Table 3
T_g values for a BTMA$^+$ BCPI, as well as for two silicate containing composites based upon the same ionomer. M_w of the BCP is 78 400 g mol^{-1} and there is 18.0 mol% styrene of which 16 mol% is sulfonated

Sample	Description	T_g (°C)	Silicate (wt%)
H	Parent BCP (control)	− 65.8	0
J	BTMA$^+$ BCPI	− 64.3	0
K	BCPI/silicate	− 64.8	6.5
L	BCPI/silicate	− 65.5	8.5

3.6. Dynamic mechanical analysis

Fig. 7(a) and (b) shows the dynamic mechanical storage and loss moduli, E' and E'', respectively, vs. temperature for a BCPI whose parent block copolymer had $M_w = 76\ 900$ g mol^{-1} and 18 mol% PS. 16 mol% of the PS blocks was sulfonated and then the sulfonic acid groups were ion exchanged with BTMA$^+$ cations. Silicate of 8.5% was then incorporated into this morphological template via the in situ sol–gel process.

In contrast with the DSC scans, the glass transition for the PS as well as the PIB phase is distinctly seen on the loss curves in Fig. 7(b). Except for transition width, the PIB phase T_g, which is considered here as temperature at the E'' maximum, is practically invariant. This suggests that neither the introduction of ions into the PS phase, nor the subsequent incorporation of silicate structures, has disrupted chain mobility in the PIB regions. This result is indirect

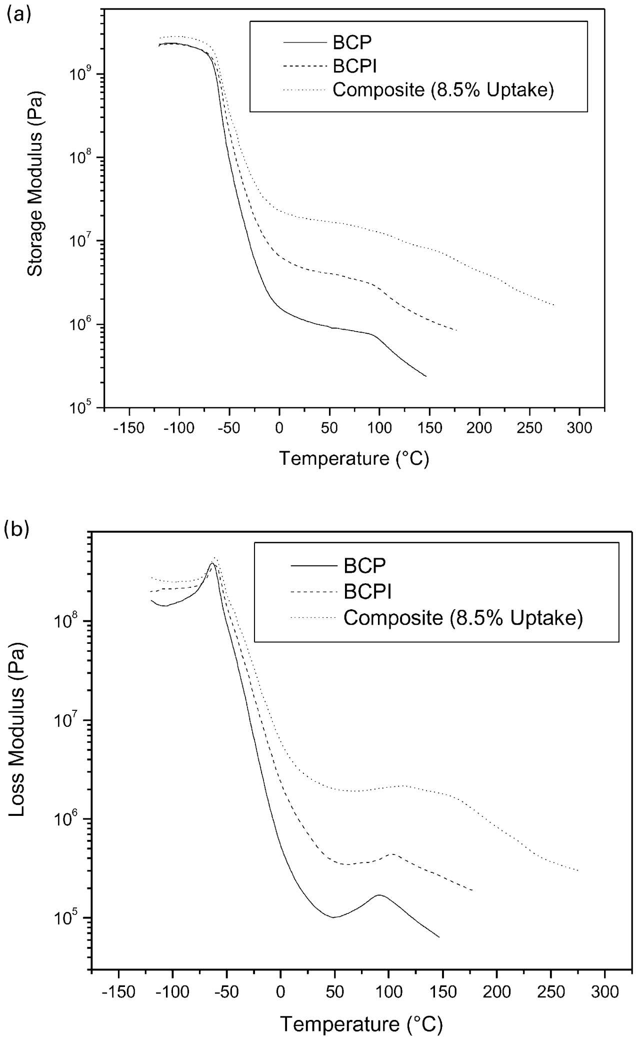

Fig. 7. (a) E' and (b) E'' vs. T for a PS–PIB–PS BCPI whose parent block copolymer had $M_w = 76\ 900$ g mol^{-1} and 18 mol% PS of which 16 mol% was sulfonated. The sulfonic acid groups were then ion exchanged with BTMA$^+$ cations and then the BCPI was imparted with 8.5% silicate.

evidence that silicate is not structured within the PIB phase, at least to an appreciable extent. On the other hand, the glass transition for the PS phase is affected by ionomer formation, and more so by silicate incorporation within the ionomer in that T_g increases in this order of BCP modification. It is reasonable to think that when ionic groups are attached to the PS blocks, the resultant strong electrostatic interactions will hinder chain mobility in these domains. PS block mobility is understandably further hindered when a rigid silicate phase is grown around and/or in these domains. While the unmodified PS block T_g is considerably elevated from ~90 °C to roughly 125 °C upon silicate incorporation, the transition is considerably broader for the latter case. This phenomenon can be viewed in terms of nanoscale heterogeneity in the dispersion of the silicate component throughout the PS domains.

Altogether, the DSC, DMA and AFM results point to a condition where the silicate phase prefers to reside in the functionalized PS domains. Thus, this in situ sol–gel process for TEOS is indeed a domain-selective process, and this particular BCPI is a rather good and robust morphological template.

In Fig. 7(a), it is seen that the rubbery plateau modulus that occurs after the PIB phase glass transition, and lies between the approximate temperatures of 0 and 100 °C, is elevated as a result of ionomer formation. The plateau modulus increases even more after the ionomer is imparted with a silicate phase. Moreover, for the BCPI/silicate hybrid, the drop in E' at around T_g for the PS blocks is not as distinctive as for the other two cases. Thus, it would seem that the insertion of only 8.5% silicate improves the mechanical integrity of these materials, which is an important consideration within the context of membrane material mechanical integrity.

4. Summary

The primary goal of these studies was to test the sol–gel polymerization template hypothesis that forms the basis of creating organic/inorganic nanocomposites via domain-targeted sol–gel reactions for metal alkoxides in phase-separated polymers. In the work presented here, the evidence suggests that we have selectively inserted silicate structures along the hard cylindrical PS domains in an ionomer form of elastomeric poly(styrene-*b*-isobutylene-*b*-styrene) tri-block copolymers via in situ sol–gel reactions for sorbed, hydrolyzed TEOS monomers. The PS blocks were first sulfonated and then ion exchanged with the organic cation BTMA to yield the ionomer form. DMAc was found to be a swelling agent that facilitates the migration of hydrolyzed $Si(OR)_4$ monomers to ionic domains where sol–gel reactions are seeded.

ESEM/EDS studies indicated that silicate structures were able to grow within the film interior rather than forming silica precipitates on the surface.

DSC and DMA studies indicated that T_g for the PIB phase is essentially unaffected, but the PS phase T_g shifts to higher values with ionomer formation, and to even higher values with subsequent silicate phase insertion. These two methods provided indirect evidence that the silicate component is mainly incorporated in the PS rather than PIB domains. This assertion is based on the view that invasive silicate nanostructures in a given phase would restrict polymer chain mobility therein. Earlier AFM studies demonstrated that the basic cylindrical morphology of the unmodified block copolymer is unchanged despite the insertion of a silicate phase [17]. The preservation of this equilibrium morphology throughout the processing steps reinforces the concept of a robust sol–gel reaction template. The rubbery plateau storage modulus was elevated as a result of ionomer formation, and more so after the ionomer was imparted with a silicate phase. Thus, the insertion of a small quantity of silicate improves the stiffness of these materials, which is important within the context of membrane integrity.

Acknowledgements

The authors gratefully acknowledge the support of the DOD EPSCoR program, administered by the Army Research Office, under grant DAAD19-99-1-0030.

References

[1] Mauritz KA. Mater Sci Engng 1998;C6:121.
[2] Juangvanich N, Mauritz KA. J Appl Polym Sci 1998;67:1799.
[3] Mauritz KA, Payne JT. J Membr Sci 2000;168:39.
[4] Young SK, Mauritz KA. J Polym Sci, Part B: Polym Phys 2001;39:1282.
[5] Siuzdak DA, Mauritz KA. J Polym Sci, B: Polym Phys 1999; 37:143.
[6] Siuzdak DA, Start PR, Mauritz KA. J Appl Polym Sci 2000;77(13):2832.
[7] Mauritz KA, Jones CK. J Appl Polym Sci 1990;40:1401.
[8] Deng Q, Cable KM, Moore RB, Mauritz KA. J Polym Sci, B: Polym Phys Ed 1996;34:1917.
[9] de Jesus MC, Weiss RA. Macromolecules 1998;31:2230.
[10] Ishizu K, Yamada Y, Saito R, Kanbara T, Yamamato T. Polymer 1992;34:2256.
[11] Chen W, Feng H, Ye C. Polym J 1997;29(2):992.
[12] Huang ZH, Dong JH, Qiu KY, Wei Y. J Appl Polym Sci 1997;66:853.
[13] Ikeda Y, Tanaka A, Kohjiya S. J Mater Chem 1997;7(8):1497.
[14] Templin M, Franck A, Du Chesne A, Leist H, Zhang Y, Ulrich R, Schaedler V, Wiesner U. Science 1997;278:1795.
[15] Brinker CJ. J Non-Cryst Solids 1988;100:31.
[16] Hench LL, Ulrich DR, editors. Ultra-structure processing of ceramics, glasses and composites New York: Wiley, 1984. p. 102.
[17] Reuschle DA, Mountz DA, Mauritz KA, Brister LB, Storey RF, Beck Tan N. Am Chem Soc Div, Polym Chem Prepr 1999;40(2):713.
[18] Mountz DA, Beck Tan N, Storey RF, Mauritz KA. Am Chem Soc Div, Polym Chem Prepr 2000;41(1):273.
[19] Lu X, Steckle WP, Weiss RA. Macromolecules 1993;26:6525.
[20] Mani S, Weiss RA, Williams CE, Hahn SF. Macromolecules 1999;32:3663.
[21] Storey RF, Brister LB. On the use of methylcyclohexane diluent for

the synthesis of polyisobutylene and poly(styrene-*b*-isobutylene-*b*-styrene) block copolymers under living cationic polymerization conditions. In preparation.

[22] Storey RF, Baugh DW, Choate KR. Polymer 1999;40:3083.

[23] Storey RF, Chisholm BJ, Lee Y. Polym Engng Sci 1997;37(1):73.

[24] Weiss RA, Sen A, Pottick LA, Willis CL. Polymer 1991;32(10):1867.

[25] Mountz DA, Reuschle DA, Mauritz KA. Am Chem Soc Div, Polym Sci Prepr 1999;40(2):713.

[26] McCrum NG, Read BE, Williams G. Anelastic and dielectric effects in polymeric solids. New York: Dover, 1991 p. 44.